

1 Proteomic insight into human directed evolution of the domesticated chicken
2 *Gallus gallus*.

3

4

5 Short Title: Domestication of the modern broiler chicken

6

7 Carl J Schmidt^{1*}, Dong Kyun Kim², G Ken Pendarvis³, Behnam Abasht¹, Fiona M
8 McCarthy^{3*§}.

9

10 ¹ Department of Animal and Food Sciences, University of Delaware, Newark, DE
11 19716 USA.

12 ² Center for Innovation in Brain Sciences, University of Arizona, Tucson AZ 85721,
13 USA

14 ³ School of Animal and Comparative Biomedical Sciences, University of Arizona,
15 Tucson AZ 85721, USA

16 Corresponding authors:

17 Fiona McCarthy

18 Email fionamcc@email.arizona.edu

19 Carl J Schmidt

20 Email: schmidtc@udel.edu

21

22 **Abstract** Chicken domestication began at least 3,500 years ago for purposes of
23 divination, cockfighting, and food. Prior to industrial scale chicken production,
24 domestication selected larger birds with increased egg production. In the mid-20th
25 century companies began intensive selection with the broiler (meat) industry
26 focusing on improved feed conversion, rapid growth, and breast muscle yield.
27 Here we present proteomic analysis comparing the Ross 708 modern broiler line
28 with the UIUC legacy line. Comparing the breast muscle proteome between
29 modern broilers and legacy lines not selected for these growth traits identifies
30 cellular processes that have responded to human directed evolution. Mass
31 spectrometry was used to identify differences in protein levels in the breast
32 muscle of 6-day old chicks from Modern and Legacy lines. The results
33 highlighted elevated levels of stress proteins, ribosomal proteins, and proteins
34 that participate in the innate immune pathway in the Modern chickens.
35 Furthermore, the comparative analyses indicated differences in the levels of
36 proteins involved in multiple biochemical pathways. In particular, the Modern line
37 had elevated levels of proteins affecting the pentose phosphate pathway, TCA
38 cycle, and fatty acid oxidation and reduced protein levels of the first phase of
39 glycolysis. These analyses provide hypotheses linking the morphometric
40 changes driven by human directed selection to biochemical pathways. The
41 results also have implications for the onset of Wooden Breast disease that arose
42 due to selection for rapid breast muscle growth and is a major problem in the
43 poultry industry.

44

45 **Introduction:** The chicken has played an important role in human culture and
46 nutrition since its domestication (1, 2). The majority of the modern chicken's
47 genome was derived from the Red Junglefowl with documented introgression of
48 alleles from the Grey, Ceylon, and Green Junglefowl (3). Early domestication
49 likely led to larger birds that matured quicker and increased egg production in
50 comparison with their wild progenitors (4, 5). The advent of modern agriculture in
51 the early 20th century led to intensive genetic selection for either meat (broiler) or
52 egg (layer) production traits in the chicken. Initial efforts selecting for increased
53 broiler mass led to accumulation of adipose tissue, probably because the
54 selection did not channel the increased level of nutrients to a particular tissue (6).
55 Ultimately, improving broiler production traits led to selection for a combination of
56 larger breast muscle mass, improved feed efficiency and rapid growth.
57 Comparative studies identifying differences between selected and unselected
58 (legacy) lines provide insight into the impact of evolution of species. Several
59 studies have characterized the differences between modern broilers and legacy
60 lines that have not been subjected to production level human directed selection
61 (7-13). In our work (14-16) we compared the modern Ross 708 broiler line and
62 the legacy University of Illinois, Urbana Campus (UIUC) lines (17, 18). In the
63 legacy line the breast muscle comprises approximately 9% of the body mass,
64 while in the modern broiler this tissue constitutes up to 22% of the body mass
65 (14). Evolving in the tropics, the jungle fowl had little need for long distance
66 flying. The wild chicken is an episodic flier, only needing the ability to fly up into a
67 tree to escape predators and to roost. Like the legacy line, the breast muscle of

68 the Red Jungle Fowl constitutes approximately 9% of its body mass (19) . For
69 comparison, the breast muscle of birds capable of more sustained flight averages
70 17% while that of hummingbirds varies between 25%-30% (20).
71 The increase in the modern broiler's breast muscle mass, which almost reaches
72 the hummingbird level, came at the expense of other tissues. For example, the
73 normalized masses of the heart, spleen and brain are larger in legacy lines
74 compared with modern broilers (13, 14, 21). In modern broilers, this likely is
75 responsible for increased incidence of cardiomyopathy (22, 23) and immune
76 deficiencies (10). The reduced brain mass in broilers could contribute to the
77 behavioral differences seen in modern broilers compared with other lines. These
78 include a reduction in movement, along with reduced fear and risk aversion in
79 comparison with legacy or layer lines (24) In addition, a myopathy called
80 Wooden Breast disease has arisen during the selection process (25-27). This
81 myopathy is apparently due to selection for rapid growth and is characterized by
82 necrosis, fibrosis, and immune cells infiltration that results in a product that is
83 unappealing to consumers (28-31). This disease results in significant losses to
84 the poultry industry as the meat is condemned at processing (32).
85 In prior work, we compared the breast muscle transcriptome of 6-day old (D6)
86 modern and legacy lines (16). That comparison identified differently expressed
87 genes affecting growth factors, lipid metabolism and the pentose phosphate
88 pathway. In particular, the modern transcriptome indicated elevated expression
89 of Insulin Like Growth Factor 1 (IGF1) which stimulates muscle hypertrophy
90 combined with reduced expression of Myostatin (MSTN), an inhibitor of skeletal

91 muscle hyperplasia (33). These studies suggest that human directed evolution
92 increased growth factor stimulation in the modern breast muscle. Furthermore,
93 elevated expression of genes involved in the pentose phosphate pathway and
94 lipid metabolism would provide necessary intermediates and energy required for
95 rapid growth.

96 Here we report a comparative study between modern Ross 708 and legacy UIUC
97 breast muscle proteomes. The results support and extend the conclusions of our
98 prior studies, providing further insight into the impact of selection that yielded
99 modern broilers (14, 16). The data also have implications for the negative effects
100 of intense selection on the broiler chicken along with the emergence of Wooden
101 Breast disease (25, 28, 29, 34, 35)

102 **Materials and Methods:**

103

104 **Animal care and sample collection:** Animal raising, handling and sample
105 collection methods were approved by the Committee on the Ethics of Animal
106 Experiments of the University of Delaware (Permit Number: 2703-12-10). Six
107 male UIUC and six male Ross 708 breast muscle samples were collected at day
108 6 post-hatch, frozen in liquid nitrogen and stored at -80°C until processed for
109 proteome analysis.

110 **Proteomic analysis:** For each of the muscle samples, six technical replicates
111 were analyzed by mass spectrometry. In each case 50 mg of each muscle
112 sample was subject to differential detergent fractionation and 20 µg of each
113 fraction was trypsin digestion as previously described (36, 37). Following
114 digestion, each fraction was desalted using a peptide macrotrap (Michrom

115 BioResources) according to the manufacturer's instructions. After desalting, each
116 fraction was further purified using a strong cation exchange macrotrap to remove
117 any residual detergent, which could interfere with the mass spectrometry.
118 Fractions were dried and resuspended in 10 μ l of 2% acetonitrile, 0.1% formic
119 acid and transferred to low retention vials in preparation for separation using
120 reverse phase liquid chromatography.

121 An Ultimate 3000 (Dionex) high performance liquid chromatography system
122 coupled with an LTQ Velos Pro (Thermo) mass spectrometer were for peptide
123 separation and mass spectrum acquisition. The U3000 was operated at a flow
124 rate of 333 nl per minute and equipped with a 75 μ m x 10 cm fused silica column
125 packed with Halo C18 reverse phase material (Mac-Mod Analytical). Each
126 peptide sample was separated using a 4 h gradient from 2% to 50% acetonitrile
127 with 0.1% formic acid as a proton source. The column was located on a
128 Nanospray Flex Ion Source (Thermo) and connected directly to a silica
129 Nanospray emitter to minimize peak broadening. High voltage was applied using
130 a stainless-steel junction between the column and the emitter. Scan parameters
131 for the LTQ Velos Pro were one MS scan followed by 10 MS/MS scans of the 5
132 most intense peaks. MS/MS scans were performed in pairs, one using collision
133 induced dissociation (CID) and the other using higher-energy collisional
134 dissociation (HCD). Dynamic exclusion was enabled with a mass exclusion time
135 of 3 min and a repeat count of 1 within 30 sec of initial m/z measurement.

136 **Protein identification:** Spectrum matching programs X!tandem (38) and
137 OMSSA (39) were used via the University of Arizona High Throughput

138 Computing Center. Raw spectra were converted to MGF format for analysis
139 using the MSConvert tool from the ProteoWizard software suite (40). X!tandem
140 was run with 12 threads, precursor and fragment tolerance of 0.2 Da, and up to
141 two missed tryptic cleavages. Variable modifications used in the searches were:
142 single and double oxidation of Methionine, carbamidomethylation of Cysteine,
143 and phosphorylation of Tyrosine, Threonine, and Serine. OMSSA was run with
144 12 threads, precursor and fragment tolerance of 0.2 Da, up to two missed tryptic
145 cleavages, and set to XML output format. A custom Perl script was used to parse
146 XML search results from both X!tandem and OMSSA. Peptides with e-values \leq
147 0.05 were accepted and single spectrum identifications were rejected unless they
148 were identified by both search engines. To verify data set quality, decoy
149 searches were performed in the exact manner as before, but with a randomized
150 version of the protein databases. False discovery rates ranged from 0.9% to
151 2.3% with an average of 1.7%.

152 **Identifying differentially expressed proteins:** Differential expression of
153 proteins between treatments was performed pairwise using peptide elution
154 profiles as described by Wright et al (41). Precursor mass spectra were extracted
155 from the raw data in MS1 format using the MSConvert software from the
156 ProteoWizard toolset. Peptide precursor m/z values were extracted from the
157 previously compiled protein identifications using Perl. Peptide intensities were
158 summed for each protein on a per-replicate basis. Data were normalized based
159 on the mode of each replicate rather than the mean to minimize the effect of
160 extreme values. A resampling analysis was performed for each pairwise

161 comparison. Proteins were considered to be differentially expressed if the
162 difference in means between conditions resulted in a P-value ≤ 0.05 .

163 **Data deposition:** Transcript data discussed in this publication have been
164 deposited in NCBI's Gene Expression Omnibus (GEO) and are accessible
165 through GEO Series accession number GSE65217. Red Jungle Fowl proteomics
166 data is available from ProteomeXchange (PXD005288). Modern Ross 708 and
167 legacy UIUC proteomics data from day 6 muscle have also been deposited to
168 ProteomeXchange (XXXX and XXXX, respectively).

169 **Results:**

170 **Proteomic Results:** In the comparison between six male day 6 modern Ross
171 708 and six male day 6 legacy UIUC breast muscle, a total of 222 differentially
172 expressed proteins were detected (p-value <0.05) with 173 enriched in modern
173 samples and 49 enriched in legacy samples. Of the 222 differentially expressed
174 proteins, 130 (57%) exhibited the same direction of enrichment as shown in an
175 earlier transcriptome study (16) (Supporting Information Table S1).

176 **Gene Ontology (GO) (42).** Muscle from legacy birds were enriched for GO terms
177 relevant to myofibers and energy production in striated muscle, along with vesicle
178 transport (Fig. 1). Muscle from modern birds were enriched for terms including
179 stress response, myofibers, translation, energy production, metabolism, vesicle
180 transport and innate immunity.

181 **Figure 1.** Gene Ontology results. Orange hexagons refer to GO terms and
182 rectangles refer to proteins differentially enriched between modern (Red) and
183 legacy (Green) chicken muscle.

184 **Stress Response:** In the comparison between modern and legacy muscle, 49
185 differentially regulated proteins were part of the stress response. Five stress
186 response proteins were elevated in the legacy breast muscle including
187 cytochrome c oxidase subunit 6A1 (COX6A1), capping actin protein (CAPZB),
188 ribosomal protein S27 (RPS27), G protein subunit beta 4 (GNB4) and DnaJ heat
189 shock protein family Hsp40 member B11 (DNAJB11). 44 stress-associated

190 proteins were elevated in the modern chicken muscle compared to the legacy
191 samples. These function in a variety of stress related processes including acting
192 as chaperones and cochaperones, responding to genotoxic stress, redox
193 regulation, and protein degradation. Among these were four proteasome subunits
194 that likely offset the increased burden of misfolded proteins due to the large
195 amount of protein synthesis required for muscle hypertrophy. Nine heat shock
196 proteins (HSPs) were also elevated in muscle from the modern line, all of which
197 function as chaperones controlling the proper folding of client proteins. Five
198 members of the TCP complex that acts as an ATP dependent chaperone
199 controlling actin folding were enriched in the modern samples. (5, 6). Four
200 isomerases responsible for controlling disulfide or proline conformation and three
201 proteins that control redox stress were also elevated in the modern line.

202 **Myofiber:** Gene expression in legacy muscle showed enrichment for several
203 myofibril proteins including Gelsolin (GSN), Troponin C (TNCC), Tropomyosin
204 (TMP1 and TMP4), Myosin Light Chain 1 (MYL1), Myomesin 2 (MYOM2),
205 Cytoskeletal Keratins (KRT5 and KRT7), and Fragile X Mental Retardation
206 Syndrome-Related Protein (FXR1). CAPZB, GSN, TNCC, TPM1 and TPM4
207 regulate the dynamics of actin filament assembly. MYL1 is a non-regulatory light
208 chain that interacts with actin in generating contraction. MYOM2 is a structural
209 component that stabilizes the M band of muscle and KRT5 and KRT7 are
210 intermediate filaments components. FXR1 controls mRNA transport and
211 translation (43). Knockdown mutations of FXR1 in mice reduce limb musculature

212 and result in early mortality (44) and recessive mutations in humans results in
213 multi-minicore myopathy (45). The transcript encoding Bridging Integrator 1
214 (BIN1) is enriched in the modern line. BIN1 protein localizes to T-tubules (46)
215 where it controls Ca^{2+} signaling (47). Mutations in BIN1 cause centronuclear
216 myopathy, which causes muscle weakness and atrophy (48-50).

217 **Translation:** The most striking contrast between modern broilers such as Ross
218 708 chickens and earlier breeds is the difference in both normalized and total
219 breast muscle yield. Some of the increase in normalized breast muscle of
220 modern broilers can be attributed to hypertrophy due to increased protein
221 synthesis (51, 52). This is consistent with the enrichment in the Ross 708 birds
222 for protein translation initiation factors and ribosomal structural proteins
223 (Supplemental Table S1 and Fig. 1). In addition to ribosomal proteins, five
224 enzymes encoding tRNA ligases were enriched in Ross 708 breast muscle
225 including: lysine–tRNA ligase (KARS), serine–tRNA ligase (SARS), glycine–tRNA
226 ligase (GARS), alanine–tRNA ligase (AARS) and bifunctional glutamate/proline–
227 tRNA ligase (EPRS). These would support the elevated protein translation
228 required for the muscle hypertrophy seen in the modern line.

229 **Glycolysis:** Muscle from the UIUC legacy line is enriched for two proteins
230 involved in glycolysis: Hexose Kinase (HK) and Phosphofructokinase (PFKM)
231 (Fig. 2). HK catalyzes the first reaction of glycolysis by phosphorylating glucose
232 while PFKM drives the commitment step to glycolysis. Elevated levels of these

233 glycolytic enzymes are consistent with the fast twitch nature of breast muscle
234 from wild chickens, which is driven by glycolysis.

235
236 **Figure 2.** Glycolysis, Pentose Phosphate Pathway and TCA cycle. Red
237 rectangles indicate enzymes enriched in the modern line while dark green
238 indicates the enzymes enriched in the legacy line.

239

240 **Pentose Phosphate Pathway (PPP):** modern line breast muscle contained
241 higher levels of the PPP enzymes transketolase (TKT) and phosphoribosyl
242 pyrophosphate synthetase (PRPS1 and PRPS2). These enzymes function in the
243 nonoxidative phase of PPP returning fructose 6 phosphate and glyceraldehyde 3
244 phosphate to glycolysis and providing ribose 5 phosphate as a precursor for
245 purine and pyrimidine synthesis (Fig. 2).

246 **TCA cycle:** The main pathway affecting energy production enriched in the
247 modern line breast muscle was the TCA cycle (Fig. 2). Most enzymes directly
248 involved in the TCA cycle were elevated in the modern line muscle, including:
249 Citrate Synthase (CS), Aconitase (ACO2), Isocitrate Dehydrogenase (IDH,
250 IDH3A, IDH3B), Dihydrolipoyllysine-residue Succinyltransferase (DLST, a
251 component of α -Ketoglutarate Dehydrogenase), Succinyl-CoA ligase (SUCL2A
252 and SUCLG1) and Fumerase (FH). The components not elevated were succinate
253 dehydrogenase (SDHA) and malate dehydrogenase (MDH). The enrichment for
254 components of the TCA cycle indicates the central role of this pathway in the

255 energy metabolism of the modern Ross 708 chickens compared with the legacy
256 UIUC birds. In addition to providing coenzymes for oxidative phosphorylation, the
257 TCA cycle provides intermediates for cataplerosis to be used as precursors for
258 nucleotides, amino acids, and lipids. Anaplerosis could be supported by elevated
259 levels of glutamic-oxaloacetic transaminase 2 (GOT2) that converts glutamate to
260 α -ketoglutarate thus allowing for replenishing TCA cycle metabolites.

261 **Beta-Oxidation:** Enzymes involved in fatty acid beta oxidation are enriched in
262 the modern birds compared with the legacy line (Figure 3). One enriched enzyme
263 is acyl-CoA dehydrogenase family member 9 (ACAD9), the rate limiting enzyme
264 in the oxidation of fatty acyl CoA. ACAD9 is responsible for introducing a *trans*
265 double bonds into palmitoyl-CoA and initiating the beta-oxidation of this common
266 lipid. Also enriched is enoyl-CoA delta isomerase 1(ECI1) which is necessary for
267 beta oxidation of unsaturated fatty acids. The transcript encoding hydroxyacyl-
268 CoA dehydrogenase (HADH) is also elevated in the modern Ross 708 muscle.
269 This enzyme acts repeatedly on lipids, sequentially removing two carbon units by
270 oxidizing a 12-carbon fatty acid to acetoacetyl-CoA. Acetyl-CoA acyltransferase 2
271 (ACAT2), also enriched in Ross 708 breast muscle, oxidizes acetoacetyl-CoA to
272 acetyl-CoA. The product of beta oxidation, acetyl-CoA, can then be metabolized
273 via the TCA cycle to generate energy, or used in anabolic reactions to support
274 rapid breast muscle growth.

275 **Fig. 3** Beta-oxidation of Saturated Fatty Acids (SFA) and Unsaturated Fatty acids
276 (USFA). Red indicates proteins that are enriched in the modern line. The step indicated

277 by the oval is repeated, sequentially removing Acetyl-CoA, until the 12 carbon Lauroyl-
278 CoA is oxidized to the 4 carbon Acetoacetyl-CoA which is oxidized to Acetyl-CoA by
279 ACAT2. Red rectangles indicate enzymes enriched in the modern line while green
280 indicates the enzymes enriched in the legacy line

281 **Amino Acid Metabolism:** In addition to TCA enzymes affecting amino acid
282 anaplerosis, modern skeletal muscle was enriched for enzymes affecting glycine,
283 lysine, and methionine metabolism. Enzymes affecting glycine impact choline
284 and creatine levels include aldehyde dehydrogenase 7 family member A1
285 (ALDH7A1), betaine—homocysteine S-methyltransferase (BHMT),
286 dimethylglycine dehydrogenase (DMDGH) and glycine amidinotransferase
287 (GATM). ALDH7A1, BHMT and DMDGH form a pathway in the conversion of
288 choline to sarcosine that is found in high concentrations in skeletal muscle.
289 Choline is a precursor to phosphatidylcholine, an important component of cellular
290 membranes. GATM is part of the pathway that mediates the interconversion
291 between creatine and glycine. Creatine is also found at high concentration in
292 muscle as it is important for energy storage as creatine phosphate. Further
293 supporting creatine phosphorylation is creatine kinase B (CKB), which is elevated
294 in modern breast muscle compared with the legacy line tissue. Three enzymes
295 enriched in the modern line are involved in S-adenosylmethionine (SAM)
296 production from methionine. These include methionine adenosyltransferase
297 (MAT1A), adenosylhomocysteinase (BHMT), and adenosylhomocysteinase
298 (AHCY). SAM functions as a universal methyl donor in biological systems.

299 **Electron Transport Chain:** Enriched in the legacy breast muscle were enzymes
300 associated with the mitochondrial respirosome. These enzymes include NADH
301 dehydrogenase (NDUFS7), cytochrome c reductases (UQCRC1, UQCRC1,
302 UQCRC2), cytochrome c oxidase (COX6A1) and ATP5C1, a component of the
303 ATP synthase central stalk. Four mitochondrial components were found enriched
304 in modern Ross 708 muscle: one subunit of the electron-transfer-flavoprotein
305 (ETFA) along with inorganic pyrophosphatase (PPA2). One NADH
306 dehydrogenase (NDUFS4) and one component of the ATPase stalk, ATP
307 synthase, H⁺ transporting, mitochondrial F_o complex subunit D (ATP5H) were
308 also elevated in the modern muscle.

309 **Vesicle and Protein Transport:** The legacy line breast muscle was enriched for
310 proteins affecting vesicle transport including: COPI coat complex subunit beta 2
311 (COPB2), transmembrane p24 trafficking protein-2 (TMED2), and Amphiphysin 1
312 (AMPH). COPB2 functions in retrograde transport from the Golgi to the ER and is
313 involved in recognition of specific vesicle cargo proteins (53). The TMED proteins
314 function in anterograde transport of vesicles from the ER to the Golgi apparatus
315 and play roles in cargo selection (9). AMPH is enriched in neural tissue where it
316 is involved in endocytosis through interaction with clathrin (54, 55). Some
317 instances of the paraneoplastic Stiff-person Syndrome (SPS) (56, 57) are due to
318 AMPH autoantibodies produced in breast and lung cancer patients. SPS is
319 characterized by muscle spasms, rigidity and hypertrophy that arise from the
320 effect of the autoantibody on nerve cells that control muscles (58). Modern Ross

321 708 breast muscle was enriched for vesicle regulatory components including:
322 Cell Division Control Protein 42 (CDC42), RAB GDP Dissociation Inhibitor
323 (GDI2), RAS-related C3 botulinum toxin substrate (RAC1) and transforming
324 protein RHOA (RHOA).

325 **Innate Immunity:** Gene Ontology analysis identified 39 proteins that function in
326 innate immunity. Two, Gelsolin (GSN) and Bridging Integrator 2 (BIN2) were
327 enriched in the legacy line breast muscle. Elevated expression of GSN is
328 associated with a decreased response to a variety of inflammatory stimuli (59-64)
329 and elevated BIN2 levels are associated with decreased phagocytic activity (65).
330 The 26 proteins enriched in the modern Ross 708 breast muscle are associated
331 with neutrophil degranulation. For example, CTSB is secreted during neutrophil
332 degranulation and degrades collagen upon release into the extracellular space
333 (66, 67). PRDX6 and RAC1, associate with and activate NADPH oxidase, a
334 major source of reactive oxygen species (68-70). RAC1 (71), RHOA (72) and
335 WD repeat domain 1 (WDR1) (73) participate in the polarization that drives
336 neutrophil migration. Birds do not have cells named neutrophils, but neutrophil
337 function is carried out by heterophils in avian species (74). It is reasonable to
338 hypothesize that the innate immunity proteins are present in heterophils within
339 the breast muscle.

340 **Discussion**

341

342 The differences between modern broilers (Ross 708) and legacy lines (UIUC),
343 arose from human directed evolution selecting for the broiler's rapid growth,
344 improved feed efficiency and increased breast muscle mass. Rapid growth is
345 evidenced in the time from hatch to market. For legacy birds grown for market,
346 that would typically take 16 weeks, while with modern birds it takes 7 weeks.
347 The improved feed efficiency arose in part from selection lengthening the
348 absorptive segments of the small intestine combined with earlier maturation of
349 the liver (14). Selection for increased breast muscle has generated modern birds
350 with more than twice the breast muscle mass of legacy lines. The proteomic
351 results presented here indicate that selection caused metabolic reprogramming
352 that supports the excessive breast muscle growth seen in the modern lines.

353 In chickens, skeletal muscle hyperplasia is thought to occur prior to hatch, and
354 the increased size of the post-hatch muscle is largely due to hypertrophy (75).

355 Hypertrophy is driven by controlling the balance between protein synthesis and
356 degradation (51, 52). The enrichment of 12 ribosomal subunit proteins, initiation
357 factors EIF3I and EIF4A4, elongation factor EEF2, along with five tRNA ligases
358 likely play an important role in the increased level of muscle hypertrophy modern
359 lines. Elevated protein synthesis could also cause the increase in stress
360 response evidenced in the modern birds. The stress proteins function in a variety
361 of processes including serving as chaperones or cochaperones, or in modulating
362 genotoxic stress, redox regulation, and protein degradation.

363 The legacy line birds exhibited enrichment for HK1 and PFKM enzymes, which
364 drive the first phase of glycolysis. PFKM catalyzes the rate limiting step of
365 glycolysis, and its enrichment would direct Glucose 6-Phosphate down the
366 glycolytic pathway. This is consistent with the typical fast-twitch breast muscle
367 fibers that are seen in birds that exhibit brief episodes of flight. In contrast,
368 modern birds are enriched in one protein (TKT) that supports the nonoxidative
369 part of the pentose phosphate pathway (PPP). The non-oxidative portion of the
370 PPP provides precursors for nucleotide synthesis and feeds glucose metabolites
371 back into glycolysis. Modern Ross 708 birds also express higher levels of
372 Phosphoribosyl Pyrophosphate Synthetase, which direct Ribose-5-Phosphate to
373 nucleotide production. The elevated level of LDHB in the Ross 708 birds is
374 expected to drive the lactate:pyruvate equilibrium towards pyruvate. This would
375 retain pyruvate for further metabolism by the TCA cycle and limit the release of
376 lactate for energy production by other tissues (76). Furthermore, glucose
377 consumption supporting the modern broiler's breast muscle has ramifications for
378 brain development. As glucose is the main energy source for the brain, diversion
379 of this nutrient to the breast muscle may cause the reduced brain growth seen in
380 modern broilers compared with legacy chicken lines or jungle fowl (13).

381 The elevated levels of multiple enzymes of the TCA cycle in the Ross 708 breast
382 muscle allows this pathway to meet demands of breast muscle hypertrophy. This
383 is supported by studies in other species implicating elevated TCA cycle activity in
384 hypertrophy. For example, enrichment of TCA metabolites was noted in a KLF10

385 mouse knockout model of soleus muscle hypertrophy (77) with similar results
386 seen in aerobic exercise induced hypertrophy in humans (78, 79). Furthermore,
387 resistance training induced hypertrophy in humans increases the activity of
388 citrate synthase, the gateway enzyme to the TCA cycle (80).

389 Several enzymes involved in lipid beta-oxidation are also elevated in birds from
390 the modern line. Elevated expression of ACAD9 is particularly informative as this
391 is the rate-limiting enzyme controlling lipid oxidation and elevated HADH activity
392 also plays a role in skeletal muscle hypertrophy (80). Increased ACAD9, HADH,
393 and other enzymes involved in lipid oxidation indicates that modern Ross 708
394 birds are using lipid metabolism, in addition to the pentose phosphate and TCA
395 pathways, to provide resources supporting expansion of the breast muscle.

396 Elevated lipid beta-oxidation in the breast muscle may have ramifications for
397 morphometric changes seen in the growth of modern broilers. For example, the
398 reduced normalized heart mass in the modern Ross 708 line compared with
399 legacy UIUC birds could cause the cardiomyopathy seen in modern broilers.
400 Also, if normalized spleen mass is viewed as a proxy for immune functions, the
401 morphometric data indicates that immune function is significantly lower in modern
402 lines compared with birds from the legacy line. Metabolically this may arise from
403 the elevated lipid use in modern Ross 708 skeletal muscle. Cardiac muscle and
404 the immune system use lipids as a major source of energy. Consequently,
405 increased competition with skeletal muscle for lipids might inhibit heart growth
406 and immune function seen in modern broilers. In addition to glucose the brain

407 also readily uses ketone bodies, such as acetoacetate, to function. The elevated
408 levels of ACAT2 in modern breast muscle may reduce the availability of ketone
409 bodies for use by the brain.

410 These data support prior studies comparing the transcriptomes of 6-day old
411 modern Ross 708 and legacy UIUC birds which concluded that the legacy line
412 breast muscle was enriched for transcripts associated with glycolysis, while the
413 transcriptome of the modern birds favored beta-oxidation (16). Additionally, TKT
414 transcripts were also elevated in a study of birds with high feed efficiency
415 compared with low feed efficiency chickens (26). Elevated levels of this enzyme
416 seen in this proteome analysis provide further support for increased expression
417 of these proteins improving feed efficiency.

418 While these samples were obtained at day 6 post-hatch, there are already
419 differences between the modern and legacy lines that have implications for the
420 development of Wooden Breast Disease (28). The elevated levels of stress
421 proteins seen in breast muscle from the modern line provide compelling evidence
422 that this tissue is undergoing a variety of stresses, likely due to its rapid growth.
423 Oxidative stress is thought to be a major contributor to the development of this
424 disease (28, 81, 82) and five of the stress responsive proteins detected in this
425 study, PIT54 (83, 84), Peroxiredoxin 1, 4 and 6 and Thioredoxin play important
426 roles in regulating oxidative stress. Gene Ontology analysis of our data also
427 detected proteins associated with neutrophils in the mammalian immune system.
428 Neutrophils are one of the earliest responders to inflammation and in birds the

429 role of these phagocytic cells is filled by heterophils (74). Histological
430 examination of birds prone to Wooden Breast Myopathy revealed heterophilic
431 infiltration in the pectoral muscle of D14 chickens and this is thought to be an
432 early sign of disease development (25). Furthermore, lipid metabolism has been
433 shown to be altered in rapidly growing broilers that develop Wooden Breast
434 Disease (85). Taken together, the proteomic data suggests that Wooden Breast
435 Disease starts to develop well before the disease is visually or palpably evident.

436 **Conclusions:** This study provides insight into the proteomic response to human
437 directed selection for broiler production traits. Elevated levels of proteins involved
438 in translation support the increased muscle hypertrophy seen in modern broilers.
439 Changes in energy production pathways including increased fatty acid oxidation,
440 diversion of glucose into the pentose phosphate pathway, retention of pyruvate
441 through the action of LDHB and elevated TCA enzymes, provide the resources
442 necessary for continued muscle growth of modern broilers. In turn, the activity of
443 these pathways in the breast muscle are likely preventing nutrients from reaching
444 other organs, thus leading to the health deficiencies and behavioral changes
445 seen in modern broilers compared with legacy lines. Also, elevation of
446 inflammatory response proteins in day 6 modern line muscle have implications
447 for the rise of myopathies during broiler selection. The data suggest that Wooden
448 Breast Disease may have its origins early in the post-hatch growth period. An
449 important future direction will be to examine the proteomes of breast muscle
450 tissue from these two lines after day 6. In addition, the identity of these

451 differentially regulated proteins can be used to generate testable hypotheses
452 regarding the regulatory mechanisms that orchestrate the changes that have
453 been introduced to the broiler chicken by human selection.

454

455 **Acknowledgments:** This projected was supported by the Agriculture and Food
456 Research Institute competitive grant (2011-67003-30228) from the United States
457 Department of Agriculture National Institute of Food and Agriculture
458
459

460 **References**

461 1. Peters J, Lebrasseur O, Irving-Pease EK, Paxinos PD, Best J, Smallman
462 R, et al. The biocultural origins and dispersal of domestic chickens. *Proc Natl
463 Acad Sci U S A.* 2022;119(24):e2121978119.

464 2. Wood-Gush DGM. A History of the Domestic Chicken from Antiquity to the
465 19th Century. *Poultry Science.* 1959;38(2):321-6.

466 3. Lawal RA, Martin SH, Vanmechelen K, Vereijken A, Silva P, Al-Atiyat RM,
467 et al. The wild species genome ancestry of domestic chickens. *BMC Biol.*
468 2020;18(1):13.

469 4. Atikuzzaman M, Sanz L, Pla D, Alvarez-Rodriguez M, Ruber M, Wright D,
470 et al. Selection for higher fertility reflects in the seminal fluid proteome of modern
471 domestic chicken. *Comp Biochem Phys D.* 2017;21:27-40.

472 5. Schutz K, Kerje S, Carlborg O, Jacobsson L, Andersson L, Jensen P. QTL
473 analysis of a red junglefowl x white leghorn intercross reveals trade-off in
474 resource allocation between behavior and production traits. *Behav Genet.*
475 2002;32(6):423-33.

476 6. Zerjal T, Härtle S, Gourichon D, Guillory V, Bruneau N, Laloë D, et al.
477 Assessment of trade-offs between feed efficiency, growth-related traits, and
478 immune activity in experimental lines of layer chickens. *Genetics Selection
479 Evolution.* 2021;53(1).

480 7. Havenstein GB, Ferket PR, Scheideler SE, Larson BT. Growth, livability,
481 and feed conversion of 1957 vs 1991 broilers when fed "typical" 1957 and 1991
482 broiler diets. *Poult Sci.* 1994;73(12):1785-94.

483 8. Havenstein GB, Ferket PR, Scheideler SE, Rives DV. Carcass
484 composition and yield of 1991 vs 1957 broilers when fed "typical" 1957 and 1991
485 broiler diets. *Poult Sci.* 1994;73(12):1795-804.

486 9. Qureshi MA, Havenstein GB. A comparison of the immune performance of
487 a 1991 commercial broiler with a 1957 randombred strain when fed "typical" 1957
488 and 1991 broiler diets. *Poult Sci.* 1994;73(12):1805-12.

489 10. Cheema MA, Qureshi MA, Havenstein GB. A comparison of the immune
490 response of a 2001 commercial broiler with a 1957 randombred broiler strain
491 when fed representative 1957 and 2001 broiler diets. *Poult Sci.*
492 2003;82(10):1519-29.

493 11. Havenstein GB, Ferket PR, Qureshi MA. Carcass composition and yield of
494 1957 versus 2001 broilers when fed representative 1957 and 2001 broiler diets.
495 *Poult Sci.* 2003;82(10):1509-18.

496 12. Havenstein GB, Ferket PR, Qureshi MA. Growth, livability, and feed
497 conversion of 1957 versus 2001 broilers when fed representative 1957 and 2001
498 broiler diets. *Poult Sci.* 2003;82(10):1500-8.

499 13. Jackson S, Diamond J. Metabolic and Digestive Responses to Artificial
500 Selection in Chickens. *Evolution.* 1996;50(4):1638-50.

501 14. Schmidt CJ, Persia ME, Feierstein E, Kingham B, Saylor WW.
502 Comparison of a modern broiler line and a heritage line unselected since the
503 1950s. *Poult Sci.* 2009;88(12):2610-9.

504 15. Zhang J, Schmidt CJ, Lamont SJ. Transcriptome analysis reveals
505 potential mechanisms underlying differential heart development in fast- and slow-
506 growing broilers under heat stress. *BMC Genomics*. 2017;18(1):295.

507 16. Davis RV, Lamont SJ, Rothschild MF, Persia ME, Ashwell CM, Schmidt
508 CJ. Transcriptome analysis of post-hatch breast muscle in legacy and modern
509 broiler chickens reveals enrichment of several regulators of myogenic growth.
510 *PLoS One*. 2015;10(3):e0122525.

511 17. Schoettle CER, EF, Norton H, Alberts J. A study of New Hampshire X
512 Barred Columbian chicks from two days of age to ten weeks of age: Effects of
513 coccidiostats. *Poultry Science*. 1956;35: 596-9.

514 18. Schoettle R, E.F., Alberts, J.O., Scott, H.M. A Study of New Hampshire X
515 Barred columbina chicks from two days of age to ten weeks of age growth, organ
516 weights. *Poultry Science*. 1956;35:95-8.

517 19. Endo H, Tsunekawa N, Kudo K, Oshida T, Motokawa M, Sonoe M, et al.
518 Comparative morphological study of skeletal muscle weight among the red jungle
519 fowl (*Gallus gallus*) and various fowl breeds (*Gallus domesticus*). *J Exp Zool B*
520 *Mol Dev Evol*. 2022;338(8):542-51.

521 20. Greenewalt CH. Dimensional relationships for flying animals. *Smithsonian*
522 *miscellaneous collections*. 1962;144:1-46.

523 21. Kawabe S, Tsunekawa N, Kudo K, Tirawattanawanich C, Akishinonomiya
524 F, Endo H. Morphological variation in brain through domestication of fowl. *J Anat*.
525 2017;231(2):287-97.

526 22. Olkowski AA, Wojnarowicz C, Laarveld B. Pathophysiology and
527 pathological remodelling associated with dilated cardiomyopathy in broiler
528 chickens predisposed to heart pump failure. *Avian Pathol.* 2020;49(5):428-39.

529 23. Olkowski AA. Pathophysiology of heart failure in broiler chickens:
530 structural, biochemical, and molecular characteristics. *Poult Sci.* 2007;86(5):999-
531 1005.

532 24. Chen S, Yan C, Xiang H, Xiao J, Liu J, Zhang H, et al. Transcriptome
533 changes underlie alterations in behavioral traits in different types of chicken.
534 *Journal of Animal Science.* 2019;98(6).

535 25. Papah MB, Brannick EM, Schmidt CJ, Abasht B. Evidence and role of
536 phlebitis and lipid infiltration in the onset and pathogenesis of Wooden Breast
537 Disease in modern broiler chickens. *Avian Pathol.* 2017;46(6):623-43.

538 26. Abasht B, Zhou N, Lee WR, Zhuo Z, Peripolli E. The metabolic
539 characteristics of susceptibility to wooden breast disease in chickens with high
540 feed efficiency. *Poult Sci.* 2019;98(8):3246-56.

541 27. Abasht B, Papah MB, Qiu J. Evidence of vascular endothelial dysfunction
542 in Wooden Breast disorder in chickens: Insights through gene expression
543 analysis, ultra-structural evaluation and supervised machine learning methods.
544 *PLoS One.* 2021;16(1):e0243983.

545 28. Abasht B, Mutryn MF, Michalek RD, Lee WR. Oxidative Stress and
546 Metabolic Perturbations in Wooden Breast Disorder in Chickens. *PLoS One.*
547 2016;11(4):e0153750.

548 29. Clark DL, Velleman SG. Spatial influence on breast muscle morphological
549 structure, myofiber size, and gene expression associated with the wooden breast
550 myopathy in broilers. *Poult Sci.* 2016;95(12):2930-45.

551 30. Velleman SG, Clark DL, Tonniges JR. The Effect of the Wooden Breast
552 Myopathy on Sarcomere Structure and Organization. *Avian Dis.* 2018;62(1):28-
553 35.

554 31. Chen LR, Suyemoto MM, Sarsour AH, Cordova HA, Oviedo-Rondon EO,
555 Wineland M, et al. Temporal characterization of wooden breast myopathy
556 ("woody breast") severity and correlation with growth rate and lymphocytic
557 phlebitis in three commercial broiler strains and a random-bred broiler strain.
558 *Avian Pathol.* 2019;48(4):319-28.

559 32. Zanetti MA, Tedesco DC, Schneider T, Teixeira STF, Daroit L, Pilotto F, et
560 al. Economic losses associated with Wooden Breast and White Striping in
561 broilers. *Semina: Ciências Agrárias.* 2018;39(2).

562 33. Hennebry A, Oldham J, Shavlakadze T, Grounds MD, Sheard P, Fiorotto
563 ML, et al. IGF1 stimulates greater muscle hypertrophy in the absence of
564 myostatin in male mice. *J Endocrinol.* 2017;234(2):187-200.

565 34. Velleman SG, Clark DL. Histopathologic and Myogenic Gene Expression
566 Changes Associated with Wooden Breast in Broiler Breast Muscles. *Avian Dis.*
567 2015;59(3):410-8.

568 35. Velleman SG, Clark DL, Tonniges JR. Fibrillar Collagen Organization
569 Associated with Broiler Wooden Breast Fibrotic Myopathy. *Avian Dis.*
570 2017;61(4):481-90.

571 36. McCarthy FM, Cooksey AM, Burgess SC. Sequential detergent extraction
572 prior to mass spectrometry analysis. *Methods Mol Biol.* 2009;528:110-8.

573 37. McCarthy FM, Cooksey AM, Wang N, Bridges SM, Pharr GT, Burgess SC.
574 Modeling a whole organ using proteomics: the avian bursa of Fabricius.
575 *Proteomics.* 2006;6(9):2759-71.

576 38. Craig R, Beavis RC. A method for reducing the time required to match
577 protein sequences with tandem mass spectra. *Rapid Commun Mass Spectrom.*
578 2003;17(20):2310-6.

579 39. Geer LY, Markey SP, Kowalak JA, Wagner L, Xu M, Maynard DM, et al.
580 Open mass spectrometry search algorithm. *J Proteome Res.* 2004;3(5):958-64.

581 40. Kessner D, Chambers M, Burke R, Agus D, Mallick P. ProteoWizard: open
582 source software for rapid proteomics tools development. *Bioinformatics.*
583 2008;24(21):2534-6.

584 41. Wright ML, Pendarvis K, Nanduri B, Edelmann MJ, Jenkins HN, Reddy
585 JS, et al. The Effect of Oxygen on Bile Resistance in *Listeria monocytogenes*. *J*
586 *Proteomics Bioinform.* 2016;9(4):107-19.

587 42. Ashburner M, Ball CA, Blake JA, Botstein D, Butler H, Cherry JM, et al.
588 Gene ontology: tool for the unification of biology. *The Gene Ontology*
589 Consortium. *Nat Genet.* 2000;25(1):25-9.

590 43. Smith JA, Curry EG, Blue RE, Roden C, Dundon SER, Rodriguez-Vargas
591 A, et al. FXR1 splicing is important for muscle development and biomolecular
592 condensates in muscle cells. *J Cell Biol.* 2020;219(4).

593 44. Mientjes EJ, Willemsen R, Kirkpatrick LL, Nieuwenhuizen IM, Hoogeveen-

594 Westerveld M, Verweij M, et al. Fxr1 knockout mice show a striated muscle

595 phenotype: implications for Fxr1p function in vivo. *Hum Mol Genet.*

596 2004;13(13):1291-302.

597 45. Estan MC, Fernandez-Nunez E, Zaki MS, Esteban MI, Donkervoort S,

598 Hawkins C, et al. Recessive mutations in muscle-specific isoforms of FXR1

599 cause congenital multi-minicore myopathy. *Nat Commun.* 2019;10(1):797.

600 46. Butler MH, David C, Ochoa GC, Freyberg Z, Daniell L, Grabs D, et al.

601 Amphiphysin II (SH3P9; BIN1), a member of the amphiphysin/Rvs family, is

602 concentrated in the cortical cytomatrix of axon initial segments and nodes of

603 ranvier in brain and around T tubules in skeletal muscle. *J Cell Biol.*

604 1997;137(6):1355-67.

605 47. Tjondrokoesoemo A, Park KH, Ferrante C, Komazaki S, Lesniak S, Brotto

606 M, et al. Disrupted membrane structure and intracellular Ca(2)(+) signaling in

607 adult skeletal muscle with acute knockdown of Bin1. *PLoS One.*

608 2011;6(9):e25740.

609 48. Nicot AS, Toussaint A, Tosch V, Kretz C, Wallgren-Pettersson C,

610 Iwarsson E, et al. Mutations in amphiphysin 2 (BIN1) disrupt interaction with

611 dynamin 2 and cause autosomal recessive centronuclear myopathy. *Nat Genet.*

612 2007;39(9):1134-9.

613 49. Bohm J, Vasli N, Maurer M, Cowling BS, Shelton GD, Kress W, et al.

614 Altered splicing of the BIN1 muscle-specific exon in humans and dogs with highly

615 progressive centronuclear myopathy. *PLoS Genet.* 2013;9(6):e1003430.

616 50. Claeys KG, Maisonobe T, Bohm J, Laporte J, Hezode M, Romero NB, et
617 al. Phenotype of a patient with recessive centronuclear myopathy and a novel
618 BIN1 mutation. *Neurology*. 2010;74(6):519-21.

619 51. Figueiredo VC, McCarthy JJ. Regulation of Ribosome Biogenesis in
620 Skeletal Muscle Hypertrophy. *Physiology (Bethesda)*. 2019;34(1):30-42.

621 52. West DW, Burd NA, Staples AW, Phillips SM. Human exercise-mediated
622 skeletal muscle hypertrophy is an intrinsic process. *Int J Biochem Cell Biol*.
623 2010;42(9):1371-5.

624 53. Eugster A, Frigerio G, Dale M, Duden R. The alpha- and beta'-COP WD40
625 domains mediate cargo-selective interactions with distinct di-lysine motifs. *Mol
626 Biol Cell*. 2004;15(3):1011-23.

627 54. Lichte B, Veh RW, Meyer HE, Kilimann MW. Amphiphysin, a novel protein
628 associated with synaptic vesicles. *EMBO J*. 1992;11(7):2521-30.

629 55. Wang LH, Sudhof TC, Anderson RG. The appendage domain of alpha-
630 adaptin is a high affinity binding site for dynamin. *J Biol Chem*.
631 1995;270(17):10079-83.

632 56. Moersch FP, Wolman HW. Progressive fluctuating muscular rigidity and
633 spasm ("stiff-man" syndrome); report of a case and some observations in 13
634 other cases. *Proc Staff Meet Mayo Clin*. 1956;31(15):421-7.

635 57. Murinson BB, Guarnaccia JB. Stiff-person syndrome with amphiphysin
636 antibodies: distinctive features of a rare disease. *Neurology*. 2008;71(24):1955-8.

637 58. Baizabal-Carvallo JF, Jankovic J. Stiff-person syndrome: insights into a
638 complex autoimmune disorder. *J Neurol Neurosurg Psychiatry*. 2015;86(8):840-
639 8.

640 59. Bucki R, Georges PC, Espinassous Q, Funaki M, Pastore JJ, Chaby R, et
641 al. Inactivation of endotoxin by human plasma gelsolin. *Biochemistry*.
642 2005;44(28):9590-7.

643 60. Bucki R, Byfield FJ, Kulakowska A, McCormick ME, Drozdowski W,
644 Namiot Z, et al. Extracellular gelsolin binds lipoteichoic acid and modulates
645 cellular response to proinflammatory bacterial wall components. *J Immunol*.
646 2008;181(7):4936-44.

647 61. Cheng Y, Hu X, Liu C, Chen M, Wang J, Wang M, et al. Gelsolin Inhibits
648 the Inflammatory Process Induced by LPS. *Cell Physiol Biochem*.
649 2017;41(1):205-12.

650 62. Lee WM, Galbraith RM. The extracellular actin-scavenger system and
651 actin toxicity. *N Engl J Med*. 1992;326(20):1335-41.

652 63. Osborn TM, Dahlgren C, Hartwig JH, Stossel TP. Modifications of cellular
653 responses to lysophosphatidic acid and platelet-activating factor by plasma
654 gelsolin. *Am J Physiol Cell Physiol*. 2007;292(4):C1323-30.

655 64. Sezen D, Bongiovanni AM, Gelber S, Perni U, Hutson JM, Skupski D, et
656 al. Gelsolin down-regulates lipopolysaccharide-induced intraamniotic tumor
657 necrosis factor-alpha production in the midtrimester of pregnancy. *Am J Obstet
658 Gynecol*. 2009;200(2):191 e1-4.

659 65. Sanchez-Barrena MJ, Vallis Y, Clatworthy MR, Doherty GJ, Veprintsev
660 DB, Evans PR, et al. Bin2 is a membrane sculpting N-BAR protein that influences
661 leucocyte podosomes, motility and phagocytosis. *PLoS One*. 2012;7(12):e52401.

662 66. Mohamed MM, Sloane BF. Cysteine cathepsins: multifunctional enzymes
663 in cancer. *Nat Rev Cancer*. 2006;6(10):764-75.

664 67. Ricaño-Ponce I, Peeters T, Matzaraki V, Houben B, Achten R, Cools P, et
665 al. Impact of Human Genetic Variation on C-Reactive Protein Concentrations and
666 Acute Appendicitis. *Front Immunol*. 2022;13:862742.

667 68. Ambruso DR. Peroxiredoxin-6 and NADPH oxidase activity. *Methods Enzymol*. 2013;527:145-67.

669 69. Filippi MD, Szczur K, Harris CE, Berclaz PY. Rho GTPase Rac1 is critical
670 for neutrophil migration into the lung. *Blood*. 2007;109(3):1257-64.

671 70. Dang PM, Cross AR, Babior BM. Assembly of the neutrophil respiratory
672 burst oxidase: a direct interaction between p67PHOX and cytochrome b558.
673 *Proc Natl Acad Sci U S A*. 2001;98(6):3001-5.

674 71. Wong K, Pertz O, Hahn K, Bourne H. Neutrophil polarization:
675 spatiotemporal dynamics of RhoA activity support a self-organizing mechanism.
676 *Proc Natl Acad Sci U S A*. 2006;103(10):3639-44.

677 72. Kunisaki Y, Nishikimi A, Tanaka Y, Takii R, Noda M, Inayoshi A, et al.
678 DOCK2 is a Rac activator that regulates motility and polarity during neutrophil
679 chemotaxis. *J Cell Biol*. 2006;174(5):647-52.

680 73. Kuhns DB, Fink DL, Choi U, Sweeney C, Lau K, Priel DL, et al.

681 Cytoskeletal abnormalities and neutrophil dysfunction in WDR1 deficiency.

682 Blood. 2016;128(17):2135-43.

683 74. Genovese KJ, He H, Swaggerty CL, Kogut MH. The avian heterophil. Dev

684 Comp Immunol. 2013;41(3):334-40.

685 75. Smith JH. Relation of Body Size to Muscle Cell Size and Number in the

686 Chicken. Poultry Science. 1963;42(2):283-90.

687 76. Hui S, Ghergurovich JM, Morscher RJ, Jang C, Teng X, Lu W, et al.

688 Glucose feeds the TCA cycle via circulating lactate. Nature. 2017;551(7678):115-

689 8.

690 77. Baroukh N, Canteleux N, Lefevre A, Dupuy C, Martias C, Presset A, et al.

691 Serum and Soleus Metabolomics Signature of Klf10 Knockout Mice to Identify

692 Potential Biomarkers. Metabolites. 2022;12(6).

693 78. Huffman KM, Koves TR, Hubal MJ, Abouassi H, Beri N, Bateman LA, et

694 al. Metabolite signatures of exercise training in human skeletal muscle relate to

695 mitochondrial remodelling and cardiometabolic fitness. Diabetologia.

696 2014;57(11):2282-95.

697 79. Konopka AR, Harber MP. Skeletal muscle hypertrophy after aerobic

698 exercise training. Exerc Sport Sci Rev. 2014;42(2):53-61.

699 80. Tang JE, Hartman JW, Phillips SM. Increased muscle oxidative potential

700 following resistance training induced fibre hypertrophy in young men. Appl

701 Physiol Nutr Metab. 2006;31(5):495-501.

702 81. Mutryn MF, Brannick EM, Fu W, Lee WR, Abasht B. Characterization of a
703 novel chicken muscle disorder through differential gene expression and pathway
704 analysis using RNA-sequencing. *BMC Genomics*. 2015;16:399.

705 82. Sihvo HK, Immonen K, Puolanne E. Myodegeneration with fibrosis and
706 regeneration in the pectoralis major muscle of broilers. *Vet Pathol*.
707 2014;51(3):619-23.

708 83. Iwasaki K, Morimatsu M, Inanami O, Uchida E, Syuto B, Kuwabara M, et
709 al. Isolation, characterization, and cDNA cloning of chicken turpentine-induced
710 protein, a new member of the scavenger receptor cysteine-rich (SRCR) family of
711 proteins. *J Biol Chem*. 2001;276(12):9400-5.

712 84. Wicher KB, Fries E. Haptoglobin, a hemoglobin-binding plasma protein, is
713 present in bony fish and mammals but not in frog and chicken. *Proc Natl Acad
714 Sci U S A*. 2006;103(11):4168-73.

715 85. Papah MB, Abasht B. Dysregulation of lipid metabolism and appearance
716 of slow myofiber-specific isoforms accompany the development of Wooden
717 Breast myopathy in modern broiler chickens. *Sci Rep*. 2019;9(1):17170.

718

719

720 **Supporting Information Table S1** Differentially expressed proteins. Symbols

721 with asterisks are ones that transcriptome data (16) supported proteome data.

722

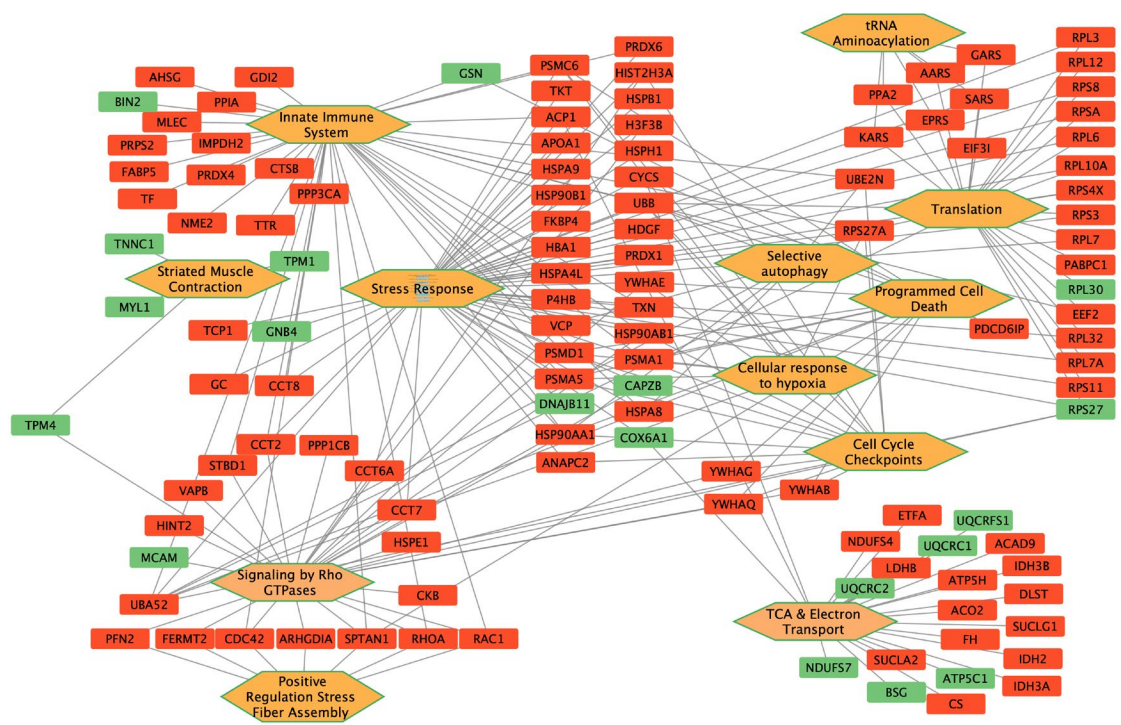


Figure 1. Functional enrichment in differentially expressed muscle. Orange hexagons refer to GO terms and rectangles refer to proteins differentially enriched between modern Ross 708 (Red) and legacy UIUC (Green) day 6 muscle.

Glycolysis

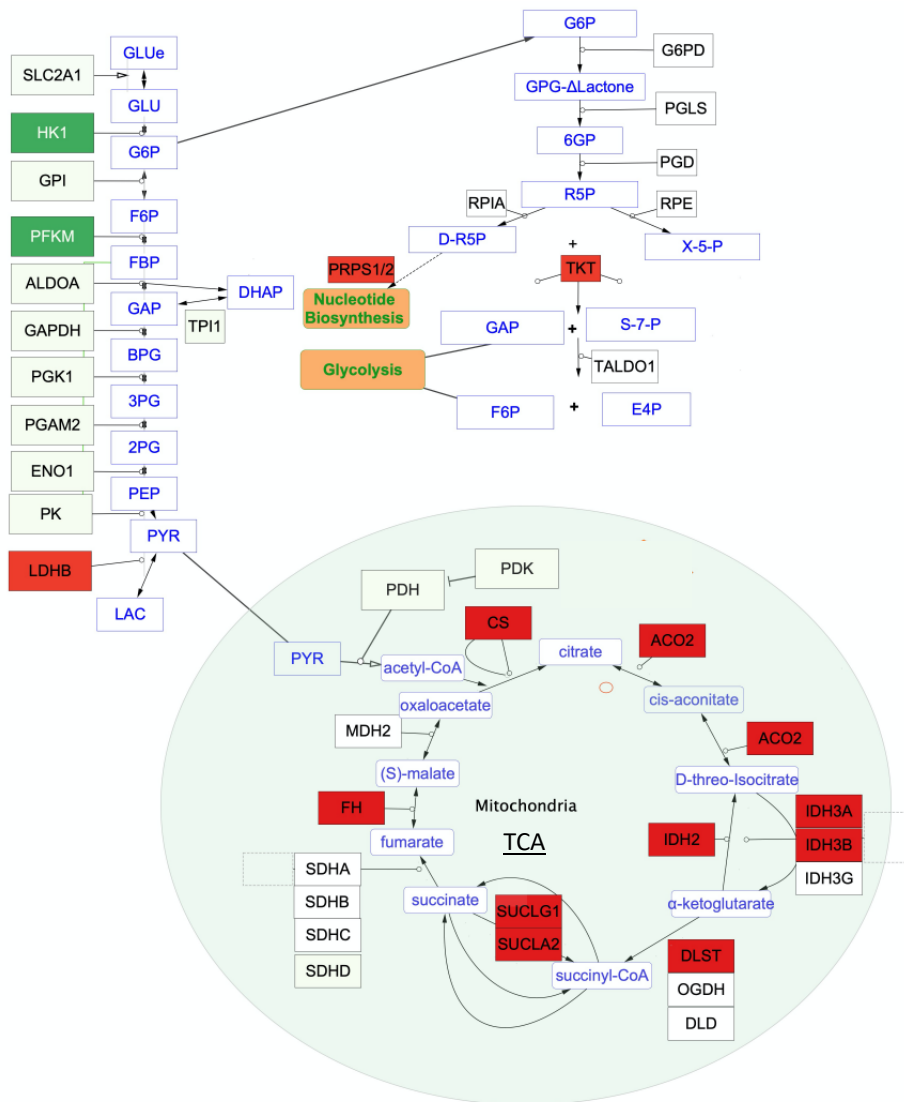


Figure 2. Glycolysis, Pentose Phosphate Pathway and TCA cycle. Red rectangles indicate enzymes enriched in modern Ross 708 chicken muscle while dark green indicates the enzymes enriched in legacy line muscle.

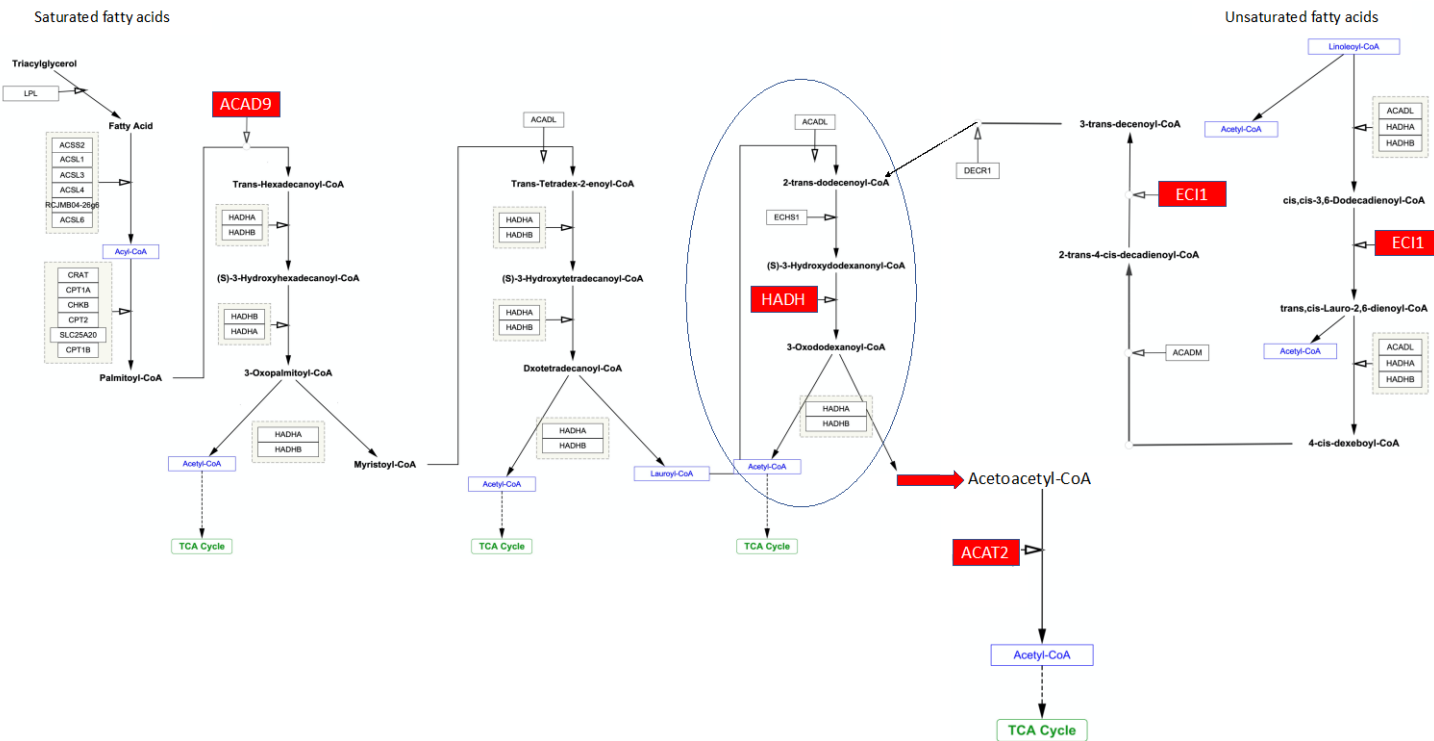


Figure 3. Beta-oxidation of Saturated Fatty Acids (SFA) and Unsaturated Fatty acids (USFA). Red indicates proteins that are enriched in modern Ross 708 muscle. The step indicated by the oval is repeated, sequentially removing Acetyl-CoA, until the 12 carbon Lauroyl-CoA is oxidized to the 4 carbon Acetoacetyl-CoA which is oxidized to Acetyl-CoA by ACAT2. Red rectangles indicate enzymes enriched in the modern Ross 708 muscle while green indicates the enzymes enriched in muscle from the legacy UIUC line.